

SHORT COMMUNICATION

Physiological and pharmacological characterization of a molluscan neuronal efflux transporter; evidence for age-related transporter impairment

Petra M. Hermann^{1,2}, Alexander C. Perry¹, Izen Hamad¹ and Willem C. Wildering^{1,3,*}

ABSTRACT

Plasma membrane efflux transporters play crucial roles in the removal and release of both harmful and beneficial substances from the interior of cells and tissue types in virtually every extant species. They contribute to the clearance of a broad spectrum of exogenous and endogenous toxicants and harmful metabolites, including the reactive lipid aldehyde byproducts of lipid peroxidation that are a hallmark of cellular ageing. Here, we tested whether declining transporter functionality may contribute to functional decline in a snail model of neuronal ageing. Through measuring the removal of 5(6)-carboxyfluorescein, a known substrate for membrane efflux transporters, we provide, for the first time, physiological evidence for the existence of probenecid-, MK571- and glutathione-sensitive efflux transporters in (gastropod) neurons and demonstrate that their functionality declines with age. Our data support the idea that waning cellular detoxification capacity might be a significant factor in the escalation of (lipo-)toxicity observed in neuronal ageing.

KEY WORDS: ABC transporter, *Lymnaea stagnalis*, Ageing, Lipid peroxidation, Probenecid, MK-571

INTRODUCTION

Cellular homeostasis, the maintenance of a balanced and stable physico-chemical intracellular environment, is critical to the functional integrity and survival of cells and, ultimately, organisms. Over the course of their lives, cells face many potentially disruptive influences arising either as a side effect of their normal functions, such as chemically reactive byproducts of their own metabolism, or as a consequence of exogenous substances such as drugs, agricultural and industrial chemicals, or other xenobiotics they absorb from their environment. Often, particularly in the case of membrane-impermeant molecules, cells respond to these kinds of challenges with extrusion of the offending substance through specialized plasma membrane transport mechanisms such as members of the highly conserved cation transporters of the solute carrier (SLC) and the ATP-binding cassette (ABC) transporter protein families (Featherstone, 2011; Höglund et al., 2011). SLC transporters function either passively or through secondary active processes and they control transmembrane movement of many types

of substrates, including neurotransmitters, metabolites, drugs and toxins (Hediger et al., 2004). ABC transporters constitute one of the largest and evolutionarily oldest families of transmembrane transporters, and representatives of most of the eight (mammalian) subfamilies are found in virtually all extant phyla (Baral, 2017; Dean et al., 2001; Dermauw and van Leeuwen, 2014; Hartz and Bauer, 2011; Jeong et al., 2017). ABC family members are expressed in most animal tissue and cell types, including neurons and glial cells of the nervous system (Abuznait and Kaddoumi, 2012; Brandmann et al., 2014; Dallas et al., 2006; Dean et al., 2001; Falcão et al., 2007; Hartz and Bauer, 2011). The majority of ABC proteins require the binding and hydrolysis of ATP to transport substrates across lipid membranes. Although many ABC transporters may mediate both influx and efflux processes, in eukaryotes they primarily facilitate efflux of unwanted molecules (Dean et al., 2001; Hartz and Bauer, 2011).

Extensive research in the biological correlates of drug resistance or uptake in cells has provided substantial insight into the function of members of the SLC and ABC subfamilies (Briz et al., 2019; DeGorter et al., 2012; Nyquist et al., 2017; Willers et al., 2019). Moreover, their role in the cellular response to environmental toxins and xenobiotics has been well described (Dermauw and van Leeuwen, 2014; Gott et al., 2017; Jeong et al., 2017). Also, although there is a growing awareness of the significance of these transporters in (age-related) neurodegenerative diseases, particularly in their functioning at the blood–brain barrier (Erdő and Krajcsi, 2019; Morris et al., 2017; Sultana and Butterfield, 2004), much less is known of their role in dealing with endogenous chemical perturbations in ageing neurons.

In this study, we investigated this question using the pond snail *Lymnaea stagnalis* (L.), a gastropod model system of neuronal ageing and age-associated learning and memory impairment (Hermann et al., 2007, 2014). Capitalizing on *L. stagnalis*'s unique large identifiable neurons, the current study investigated non-pathological, age-associated functional changes of a glutathione-dependent, probenecid- and MK-571-sensitive efflux transporter functionality.


MATERIALS AND METHODS

Animal populations

Snails were bred and raised as described before under constant and strictly controlled conditions in the laboratory (Hermann et al., 2007; Watson et al., 2012a). Briefly, they were raised at a maximal density of 1.5 snails per liter, on a 12 h:12 h light:dark cycle, at an ambient temperature of 19–20°C and fed *ad libitum* with lettuce and Aquamax-carnivorous Grower 600 trout pellets (Purina Mills LLC, St Louis, MO, USA). The facility uses reverse osmosis water that has been subsequently reconditioned to a conductivity of ~450 $\mu\text{S cm}^{-1}$ by adding Instant Ocean salts (Aquarium Systems

¹Department of Biological Sciences, Faculty of Science, University of Calgary, Calgary, AB, Canada T2N 1N4. ²Department of Physiology and Pharmacology, Cumming School of Medicine, University of Calgary, Calgary, AB, Canada T2N 4N1. ³Hotchkiss Brain Institute, University of Calgary, Calgary, AB, Canada T2N 4N1.

*Author for correspondence (wildering@ucalgary.ca)

 P.M.H., 0000-0003-0555-2325; W.C.W., 0000-0001-9120-5930

USA) at 1 g per US gallon (~3.8l). Calcium carbonate (light powder; EMD Millipore) and sterilized cuttlefish bone were added to the water to maintain a pH of 7.4–7.6 and to keep dissolved calcium concentrations at saturation level (see Johnston et al., 2017, for details of water composition). Survival characteristics of the populations were continuously monitored and evaluated using previously established methods based on the two-parameter Weibull failure model (Janse et al., 1988; Slob and Janse, 1988). Experimental animals were taken at random from differently aged populations meeting Weibull parameters consistent with healthy ageing. For the purpose of this study, old animals (20–24 months of age) are defined as animals sampled from populations with a survival percentage of 20% or less, whereas young sexually mature animals (7–9 months of age) were taken from populations with survival rates of 95% or better.

Neuronal dye labelling

The central nervous system (CNS) was dissected from anaesthetized animals (Watson et al., 2012b) and pinned down in an elastomeric-covered dish filled with a HEPES-buffered saline (HBS; for composition, see below). The large identified neuron RPD1 (right parietal dorsal 1; Fig. 1A) was impaled with a microelectrode without the use of proteolytic enzymes (Hermann and Bulloch, 1998; Hermann et al., 1997). Microelectrodes were pulled from borosilicate glass (TW150F, World Precision Instruments, Sarasota, FL, USA) and filled with 5(6)-carboxyfluorescein (CF; 4% w/v) dissolved in 0.5 mol l⁻¹ potassium acetate (CH₃COOK)/0.01 mol l⁻¹ KCl. Intra-somatal iontophoretic injection of CF was done through a 30 min pulse protocol of hyperpolarizing square current pulses with duration 500 ms, amplitude 1 nA and repetition rate of 1 Hz generated with a Model 2100 isolated pulse stimulator (A-M Systems, Sequim, WA, USA) and delivered through standard intracellular microelectrode techniques with the aid of an Axoclamp 2A amplifier (Axon Instruments, Burlingame, CA, USA; Fig. 1B).

Image acquisition and analysis

After injection of CF into the soma of RPD1, dye extrusion was monitored for 3 h (unless indicated otherwise), with sets of five images acquired at a rate of 12 h⁻¹ for the first hour, 4 h⁻¹ during the next hour and 2 h⁻¹ during the third and last hour. Exposure time of individual images was 100 ms. Gain settings were optimized for each experiment. Average fluorescence intensity for each of the sets was calculated as the arithmetic mean of each quintuplet (ImageJ version 1.51j8, NIH, Bethesda, MD, USA). Images were taken with an MVX10 macro zoom fluorescence stereomicroscope (Olympus) with 495 nm excitation/519 nm emission and a Retiga Exi-blue cooled CCD camera (QImaging, Surrey, BC, Canada) controlled through CellSense Dimensions Imaging software (v1.6, Olympus Life Science).

Chemicals and solutions

Unless stated otherwise, chemicals were obtained from Sigma Aldrich (St Louis, MO, USA) and dissolved in HBS. CF (Acros Organics, Branchburg, NJ, USA) was dissolved in microelectrode medium (0.5 mol l⁻¹ potassium acetate/0.01 mol l⁻¹ potassium chloride) to a concentration of 4% with pH set at ~7.5 with 5 mol l⁻¹ NaOH, and subsequently filtered through a 0.45 µm syringe filter. ABC transporter inhibitors MK-571 and probenecid (water-soluble; Molecular Probes, Eugene, OR, USA), γ-glutamylcysteine synthetase inhibitor buthionine sulphoximine (BSO) and membrane-permeable ethyl ester of reduced glutathione

(GSH-EE) were dissolved in HBS at concentrations indicated in the text. Adenosine 5'-triphosphate disodium salt hydrate (ATP) was dissolved in microelectrode medium to a concentration of 10 mmol l⁻¹ and co-injected with CF into the soma of RPD1 as described before (note: to monitor the efficacy of ATP delivery, electrical activity of the injected neurons was monitored for changes indicative of closure of K_{ATP} background channels; Fathi-Moghadam and Winlow, 2019). Isolated CNS was placed in saline, BSO, MK-571 or probenecid starting 30 min before impalement; treatment with GSH-EE started 60 min before impalement. All drug applications continued during dye loading and imaging. All experiments were performed in HBS (pH 7.9) with the following composition (in mmol l⁻¹): 51.3 NaCl, 1.7 KCl, 4.1 CaCl₂, 1.5 MgCl₂ and 10 Hepes.

Data analysis and statistics

Using least-squares non-linear regression techniques, one-phase exponential decay models [$Y_t = (Y_0 - Y_\infty)e^{-kt} + Y_\infty$; where Y_t is the concentration of dye remaining at time t , Y_0 is the value of Y at $t=0$, k is a rate constant and Y_∞ is the asymptotic steady-state value] were fitted to averaged CF fluorescence intensity decay time series. To deal with slight variations in loading efficacy, the models were fitted to data normalized to the mean intensity of the first frame (i.e. $Y_0=1$). Statistical significance was tested using Student's t -test or one-way ANOVA followed by Dunnett's or Šidák's multiple comparisons test where specific hypothesis tests were required. All analyses were performed and all figures made with GraphPad Prism (version 8.0.1, GraphPad Software Inc., La Jolla, CA, USA). All data are represented as arithmetic mean and s.e.m.

RESULTS AND DISCUSSION

Characterization of a neuronal efflux transporter

To monitor the activity of the neuronal efflux transporter(s) in *L. stagnalis* CNS, we iontophoretically injected the anionic fluorescent dye CF directly into the cytosol of RPD1, thereby circumventing potential (age-associated) variance in probe loading and subcellular compartmentalization commonly associated with esterified-probe loading protocols. Intracellular CF fluorescence intensity in RPD1 from young snails decayed with a single-exponential time course with half-times in the low twenties of minutes (Fig. 1C). In the absence of inhibitors, mean intracellular fluorescence intensity level declined exponentially to 21±1% of its starting value in 60 min ($n=6$, $R^2=0.9846$; Fig. 1B,C). Treatment with the anion transport inhibitors probenecid or MK-571 slowed CF fluorescence decay in a dose-dependent manner (Fig. 1B–D). Both probenecid and MK-571 displayed steep dose–effect characteristics with an IC₅₀ of 189±51.9 µmol l⁻¹ and 3.3±0.85 µmol l⁻¹, respectively (Fig. 1D), values consistent with or even below previously reported data in mammalian and other invertebrate cells and tissues (Campos et al., 2014; Della Torre et al., 2014; Gekeler et al., 1995; Renes et al., 1999; Salerno and Garnier-Suillerot, 2001). Treatment with maximal doses of probenecid (10 mmol l⁻¹, $n=11$) or MK-571 (300 µmol l⁻¹, $n=6$) linearized fluorescence-loss curves and slowed down decay rates to values as low as $-1.3(\pm 0.021) \times 10^{-3} \text{ min}^{-1}$ and $-1.6(\pm 0.014) \times 10^{-3} \text{ min}^{-1}$, respectively. Importantly, in both instances, residual fluorescence intensity levels declined to only 91±2% and 90±6% of their initial values after undergoing 60 min of exactly the same sampling protocol and exposure conditions to the untreated preparations (Fig. 1C), indicating that photobleaching had little or no effect on the disappearance of CF fluorescence in the latter preparations.

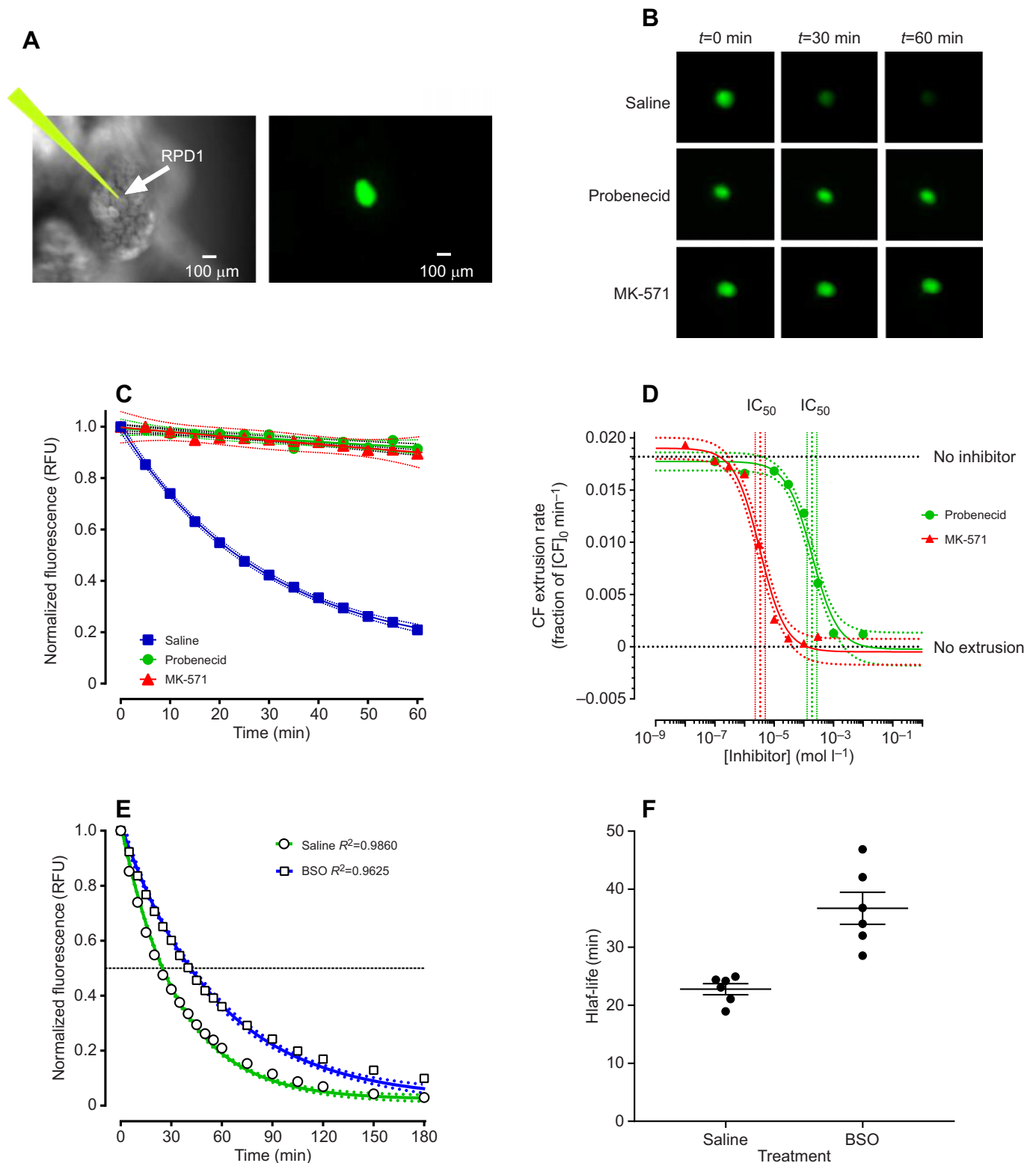


Fig. 1. Characterization of an efflux transporter in a *Lymnaea stagnalis* neuron. (A) Photographic example of the location (left) of RPD1 and fluorescence (right) after intra-somatal injection with 5(6)-carboxyfluorescein (CF). (B) Photographic time series of RPD1 CF fluorescence in either saline alone (control) or saline plus the ABC transporter inhibitors probenecid or MK-571. (C) Average change over time in normalized RPD1 CF fluorescence in the absence (saline) or presence of probenecid (10 mmol l^{-1}) or MK-571 ($300 \mu\text{mol l}^{-1}$). Note the relatively stable fluorescence levels in the presence of the ABC inhibitors. (D) Dose–response curves of the effect of probenecid and MK-571 on CF extrusion rate. IC_{50} is indicated by the vertical dotted red (MK-571) and green (probenecid) lines. (E) Average single-exponential CF fluorescence decline in RPD1 from young snails under control (saline) conditions or in the presence of the γ -glutamylcysteine synthetase inhibitor BSO. Note the significant slow-down of extrusion in the presence of BSO. (F) Scatter plot of half-life of CF fluorescence in saline or in the presence of BSO (means \pm s.e.m.). RFU, relative fluorescence units.

Together, the above results show that RPD1 express an efflux transporter with a pharmacological profile characteristic of ABCC transporters (Hagos et al., 2017; Yamazaki et al., 2005). Parenthetically, it is important to note that CF is a known substrate for members of the ABCC subfamily (Da Costa et al., 2018; Valdez et al., 2017; Van der Kolk et al., 1998).

Postulating involvement of an ABC transporter sharing characteristics with the ABCC subfamily, we tested GSH dependency of CF extrusion (Bachhawat et al., 2013; Ballatori et al., 2009; Cole and Deeley, 2006). To this end, CNS isolated from young animals was preincubated with the γ -glutamylcysteine synthetase inhibitor BSO (10 mmol l⁻¹; $n=6$). As shown in Fig. 1E, pretreatment with BSO significantly slowed down CF extrusion, yielding a (mean \pm s.e.m.) first-order decay rate constant of 0.019 \pm 0.001 RFU min⁻¹ compared with 0.031 \pm 0.001 RFU min⁻¹ under control conditions (Student's $t=5.72$, $P<0.001$, d.f.=10; $R^2_{\text{saline}}=0.9860$; $R^2_{\text{BSO}}=0.9625$), corresponding to an increase in average fluorescence intensity half-life from 22.8 \pm 0.95 min to 36.7 \pm 2.76 min (Fig. 1F; Student's $t=4.79$, $P<0.001$, d.f.=10), thus corroborating the hypothesis that CF extrusion in RPD1 is mediated by a transporter sharing defining pharmacological and physiological traits with the ABCC subfamily. A *L. stagnalis* transcriptome data search indicated that *L. stagnalis* expresses a large variety of ABC transporter homologues, including six members of the ABCC subfamily (ABCC1–5 and ABCC12; Bouétard et al., 2012; Rosenegger et al., 2010). At least two MK571 and probenecid-sensitive ABCC member homologues (ABCC1 and ABCC4) seem to be expressed in *L. stagnalis* CNS (Feng et al., 2009). Although the existence of mammalian neuronal ABCC efflux transporters has been reported before (Brandmann et al., 2014; Falcão et al., 2007; Grube et al., 2018), the data presented here provide the first physiological and functional evidence for the existence of such an efflux transporter in non-mammalian neurons.

Dye-extrusion rate declines with age

In the light of our earlier work on functional and metabolic decline of the ageing *L. stagnalis* CNS (Lee, 2019; Hermann et al., 2014; Watson et al., 2012a, 2013), we examined whether neuronal CF extrusion capacity declines with age. To this end, the disappearance of CF fluorescence from RPD1 in the CNS of six young and eight old snails was measured and analysed as above (Fig. 2A). Again, the time course of CF fluorescence decline followed single-exponential kinetics (Fig. 2B; $R^2_{\text{young}}=0.9860$; $R^2_{\text{old}}=0.9701$). However, fluorescence intensity levels declined significantly faster in young neurons than in old neurons, with average decay rate constants of 0.031 \pm 0.001 RFU min⁻¹ and 0.022 \pm 0.001 RFU min⁻¹ in young and old preparations, respectively (Fig. 2A,B; Student's $t=4.044$, $P=0.016$, d.f.=12), corresponding to an increase in fluorescence half-life from 22.8 \pm 0.95 min to 32.4 \pm 1.81 min, respectively (Fig. 2C; Student's $t=4.29$, $P=0.001$, d.f.=12). Intriguingly, both decay rate constants and half-life of old RPD1 are similar to those reported above for the BSO-treated young RPD1 (cf. Figs 1F and 2C). Importantly, treatment with 10 mmol l⁻¹ probenecid reduced fluorescence decay in both young and old preparations to the same minimal rate (Fig. 2D; ANOVA $F_{3,29}=217.8$, $P<0.0001$; Šidák's multiple comparisons tests: young versus old, $t_4=2.71$, $P<0.04$; young versus young+probenecid $t_4=19.68$, $P<0.001$; old versus old+probenecid $t_4=16.07$, $P<0.001$; young+probenecid versus old+probenecid $t_4=1.05$, $P=0.76$). Thus, after 60 min, fluorescence levels were similar in young and old preparations, and still at 91 \pm 2% and 88 \pm 3%, respectively, of their initial values (Fig. 2D). Again, this indicates that photobleaching or other processes potentially

quenching CF fluorescence (Elliott and Kleindienst, 1990; Song et al., 1995) had little or no effect on the current results. Consequentially, the marked slow-down in CF fluorescence decay of older neurons presumably involves an age-associated decline in the extrusion capacity of the probenecid/MK-571-sensitive plasma membrane efflux transporter(s).

GSH and/or ATP supplementation do not affect transporters in aged neurons

All classes of ABC transporters operate at the expense of ATP and some also require GSH (Cole and Deeley, 2006). As we demonstrated above, RPD1's CF transporter belongs to the latter group. As reported previously, GSH and ATP supplies are diminishing in ageing *L. stagnalis* neurons (Lee, 2019; Watson et al., 2014), prompting us to test the effect of ATP, GSH or ATP plus GSH supplementation on CF extrusion rates in old RPD1. Fig. 3A,C illustrates that compared with saline-only controls, neither supplementation of intracellular GSH by means of GSH-EE (10 mmol l⁻¹, $n=6$) or injection of ATP (10 mmol l⁻¹, $n=7$) effected significant changes in CF fluorescence decay kinetics (Fig. 3A–D). As before, the fluorescence decay curves were fitted very well by single-exponential decay models ($R^2_{\text{saline}}=0.9701$; $R^2_{\text{GSH-EE}}=0.9651$; $R^2_{\text{ATP}}=0.9742$) with mean decay rates of 0.022 \pm 0.001 RFU min⁻¹, 0.019 \pm 0.002 RFU min⁻¹ and 0.025 \pm 0.002 RFU min⁻¹ for saline-only, GSH-EE-treated or ATP-injected preparations, respectively. These decay rates did not differ significantly from each other (ANOVA $F_{3,23}=3.694$, $P=0.026$; Dunnett's test: saline-only versus GSH-EE, $Q=1.245$, $P=0.481$, d.f.=23; saline-only versus ATP, $Q=1.044$, $P=0.615$, d.f.=23). Likewise, CF fluorescence decay in cells that received the GSH/ATP combination treatment (Fig. 3E) could be fitted very well with a single-exponential decay model ($R^2_{\text{GSH+ATP}}=0.9856$) with a mean decay rate of 0.017 \pm 0.001 RFU min⁻¹. Notably, the combined treatment also failed to reverse the slow-down of CF extrusion in older RPD1 (Fig. 3F). In fact, the data suggest that even though this effect was not statistically significant, the combined treatment may cause CF extrusion to decelerate even further (ANOVA $F_{3,23}=3.694$, $P=0.026$; Dunnett's test: saline-only versus GSH/ATP, $Q=2.177$, $P=0.1023$, d.f.=23).

Together, these results show that enhancing intracellular GSH and/or ATP levels does not return old neurons to the higher CF extrusion rates characteristic of young neurons. Importantly, indicative of successful delivery of both compounds, we noticed resting membrane potential depolarization and/or increased electrical activity of injected RPD1 in all cases (data not shown). Previous studies have shown that intracellular ATP concentrations ([ATP]_i) >2 mmol l⁻¹ are required to inhibit ATP-sensitive background potassium channels in *L. stagnalis* neurons underlying this ATP response (Fathi-Moghadam and Winlow, 2019; Lozovaya et al., 1993). Moreover, normal cytosolic ATP concentration in (mammalian) neurons is estimated to be between 1 and 3 mmol l⁻¹ (Ainscow et al., 2002; Chinopoulos et al., 2000; Pathak et al., 2015; Rangaraju et al., 2014). Thus, even though we could not measure final [ATP]_i in our experiments, ATP injections probably increased [ATP]_i in excess of 1–2 mmol l⁻¹.

Our results raise the question why probenecid/MK-571-sensitive efflux transporter capacity of *L. stagnalis* neurons declines with age. We can as yet not answer this question with certainty. However, several studies have shown an age-related attenuation of expression levels of efflux transporters (including ABC transporters) located at the blood–brain barrier (Erdő and Krajcsi, 2019; Erickson and Banks, 2019). Hence, it is conceivable that the CF efflux transporter capacity of RPD1 is affected by an age-associated decline in

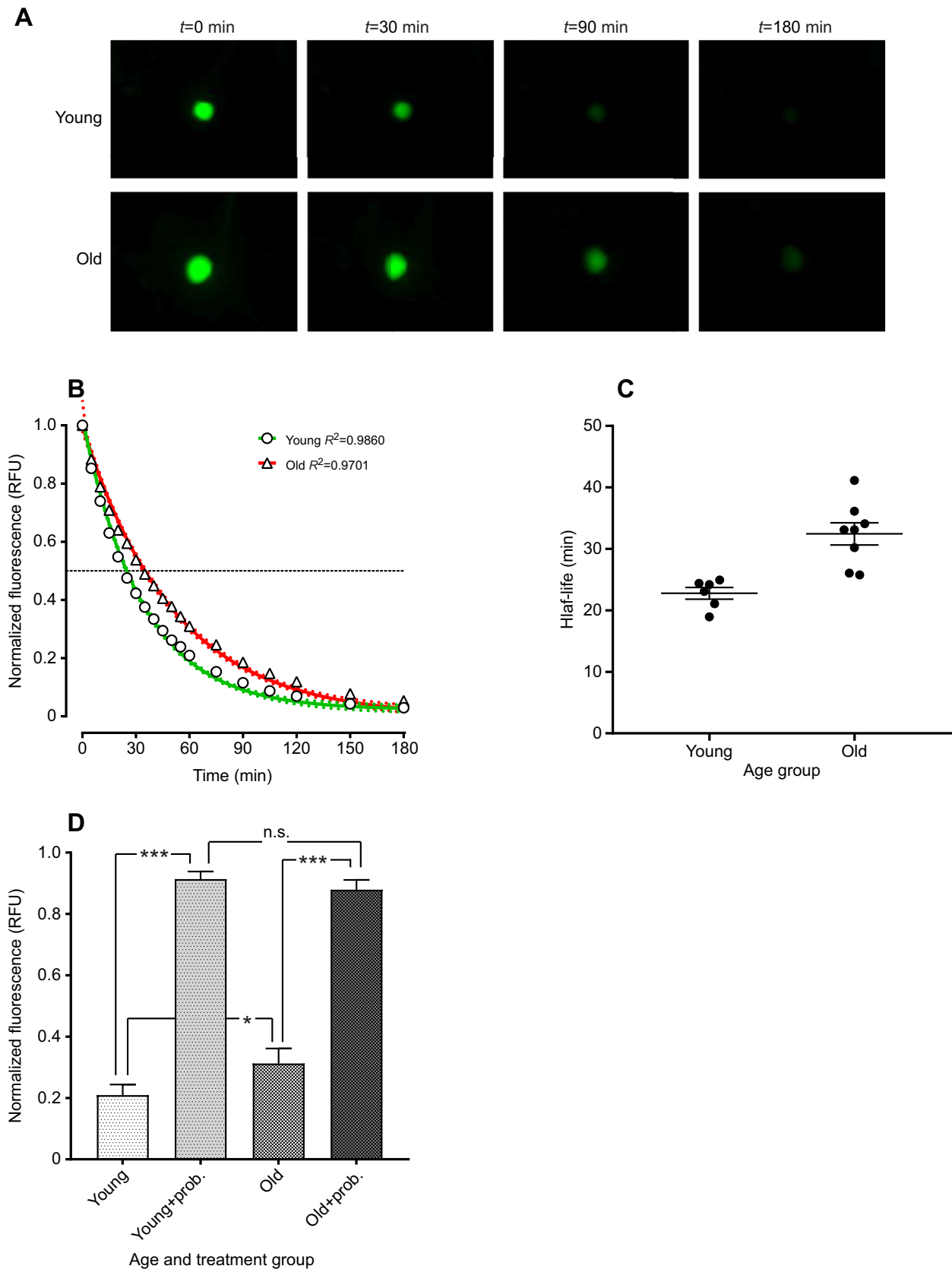


Fig. 2. Age-associated reduction in efflux transporter functioning. (A) Time series of CF fluorescence decay in RPD1 from young and old snails. (B) Average single-exponential CF fluorescence decline in RPD1 of young and old animals. Note the significant slow-down of dye extrusion in old RPD1. (C) Scatter plot of half-life of CF fluorescence in young and old RPD1 (means \pm s.e.m.). (D) Average CF fluorescence after 60 min of saline or probenecid treatment in young and old RPD1. Note that probenecid treatment prevents dye extrusion in both young and old preparations to the same extent. * $P < 0.05$, *** $P < 0.001$; n.s., not significant; RFU, relative fluorescence units.

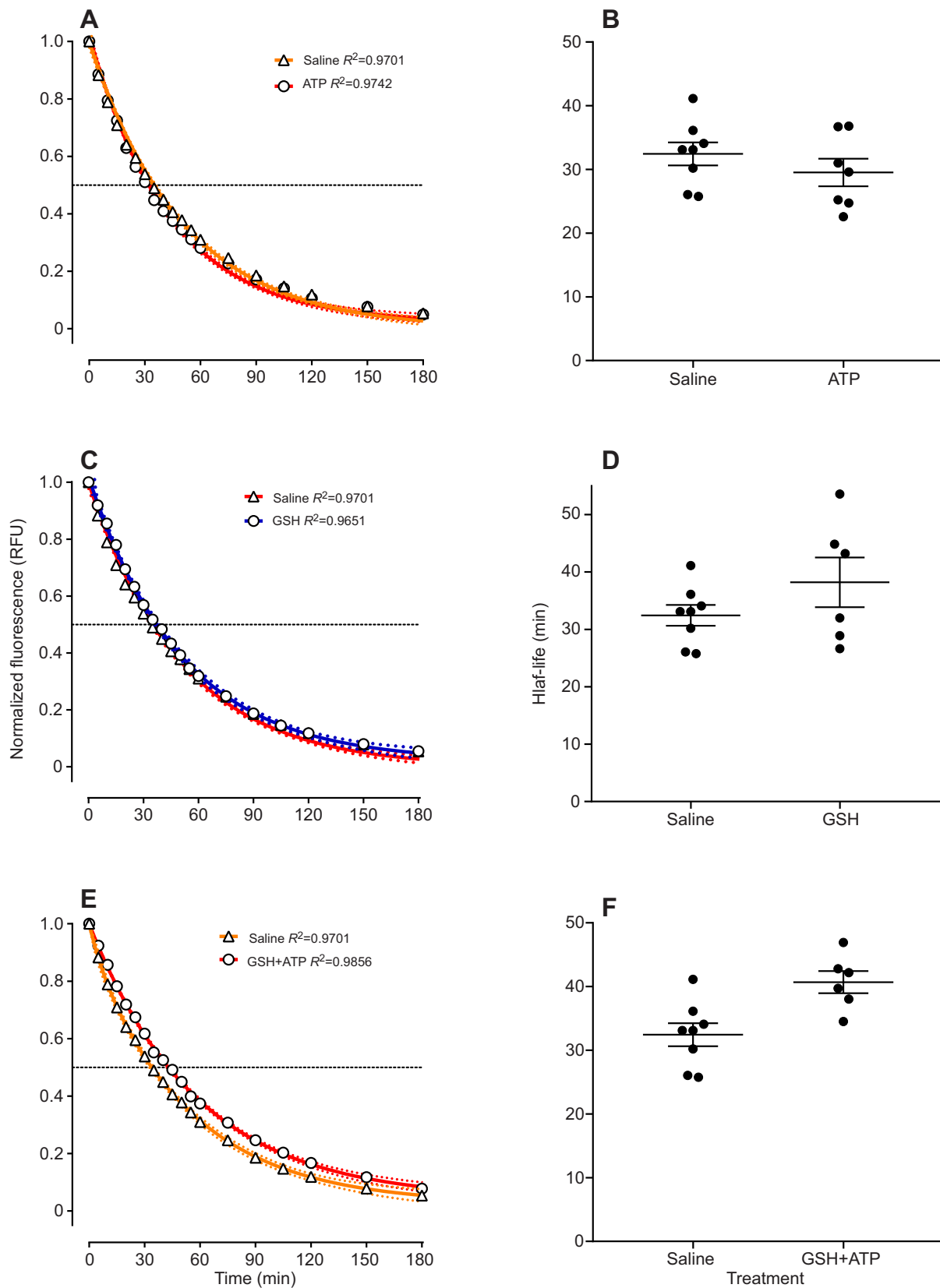


Fig. 3. GSH and/or ATP supplementation does not accelerate extrusion rate in old neurons. (A) Average CF fluorescence decay time series in old RPD1 with and without treatment with ATP. (B) Scatter plot of CF fluorescence half-life in old RPD1 with or without ATP injection (means \pm s.e.m.). (C) Average CF fluorescence decay time series in old RPD1 in saline or with membrane-permeable ethyl ester of reduced glutathione (GSH-EE). (D) Scatter plot of CF fluorescence half-life in old RPD1 in saline or with GSH-EE (means \pm s.e.m.). (E) Average single-exponential CF fluorescence decline in old RPD1 in saline or with a combination of ATP and GSH-EE. (F) Scatter plot of CF fluorescence half-life in old RPD1 in saline or a combination of ATP and GSH-EE (means \pm s.e.m.). RFU, relative fluorescence units.

transporter protein expression. Alternatively, many ABC transporter proteins, including members of the ABCC subfamily, possess redox-sensitive cysteine residues, the oxidation of which under oxidative stress conditions disrupts their transporter activity (Kuo, 2009). Hence, age-associated escalation of oxidative stress, one of the hallmarks of ageing in the vast majority of model systems including the *L. stagnalis* nervous system, may contribute to the phenomena reported here (Hermann et al., 2014; Watson et al., 2012a). Last but not least, considering the important role ABC(C) transporters play in the removal of toxic endogenous compounds including reactive lipid aldehydes, reduced efflux capacity might lead to an accumulation of these compounds and as a result further negatively affect the functioning of these transporters (Ji et al., 2002; Jungsuwadee et al., 2006; Renes et al., 2000; Sultana and Butterfield, 2004; Zhang and Forman, 2017).

In conclusion, the results presented here provide evidence that functioning of an efflux transporter, with the pharmacological characteristics of an ABCC-like transporter, attenuates with age in *L. stagnalis* neurons and furthers our theory that declining cellular detoxification capacity is a factor in the functional decline of normal ageing neurons.

Competing interests

The authors declare no competing or financial interests.

Author contributions

Conceptualization: P.M.H., W.C.W.; Methodology: P.M.H., A.C.P.; Validation: P.M.H., W.C.W.; Formal analysis: P.M.H., W.C.W.; Data curation: P.M.H., A.C.P., I.H.; Writing - original draft: P.M.H., W.C.W.; Writing - review & editing: P.M.H., W.C.W.; Supervision: W.C.W.; Funding acquisition: W.C.W.

Funding

The work was supported by a National Science and Engineering Research Council of Canada (NSERC) operating grant to W.C.W.

References

- Abuznait, A. H. and Kaddoumi, A. (2012). Role of ABC transporters in the pathogenesis of Alzheimer's disease. *ACS Chem. Neurosci.* **3**, 820-831. doi:10.1021/cn300077c
- Ainscow, E. K., Mirshamsi, S., Tang, T., Ashford, M. L. J. and Rutter, G. A. (2002). Dynamic imaging of free cytosolic ATP concentration during fuel sensing by rat hypothalamic neurones: evidence for ATP-independent control of ATP-sensitive K⁺ channels. *J. Physiol.* **544**, 429-445. doi:10.1113/jphysiol.2002.022434
- Bachhawat, A. K., Thakur, A., Kaur, J. and Zulkifli, M. (2013). Glutathione transporters. *Biochim. Biophys. Acta.* **1830**, 3154-3164. doi:10.1016/j.bbagen.2012.11.018
- Ballatori, N., Krance, S. M., Marchan, R. and Hammond, C. L. (2009). Plasma membrane glutathione transporters and their roles in cell physiology and pathophysiology. *Mol. Aspects Med.* **30**, 13-28. doi:10.1016/j.mam.2008.08.004
- Baral, B. (2017). Evolutionary trajectories of entomopathogenic fungi ABC transporters. *Adv. Genet.* **98**, 117-154. doi:10.1016/bs.adgen.2017.07.002
- Bouéard, A., Noirot, C., Besnard, A. L., Bouchez, O., Choisine, D., Robe, E., Klopp, C., Lagadic, L. and Coutellec, M. A. (2012). Pyrosequencing-based transcriptomic resources in the pond snail *Lymnaea stagnalis*, with a focus on genes involved in molecular responses to diquat-induced stress. *Ecotoxicol.* **21**, 2222-2234. doi:10.1007/s10646-012-0977-1
- Brandmann, M., Hohnholt, M. C., Petters, C. and Dringen, R. (2014). Antiretroviral protease inhibitors accelerate glutathione export from viable cultured rat neurons. *Neurochem. Res.* **39**, 883-892. doi:10.1007/s11064-014-1284-4
- Briz, O., Perez-Silva, L., Al-Abdulla, R., Abete, L., Reviejo, M., Romero, M. R. and Marin, J. J. G. (2019). What "The Cancer Genome Atlas" database tells us about the role of ATP-binding cassette (ABC) proteins in chemoresistance to anticancer drugs. *Expert Opin. Drug Metab. Toxicol.* **15**, 577-593. doi:10.1080/17425255.2019.1631285
- Campos, B., Altenburger, R., Gómez, C., Lacorte, S., Piña, B., Barata, C. and Luckenbach, T. (2014). First evidence for toxic defense based on the multidrug resistance (MDR) mechanism in *Daphnia magna*. *Aquat. Toxicol.* **148**, 139-151. doi:10.1016/j.aquatox.2014.01.001
- Chinopoulos, C., Tretter, L., Rozsa, A. and Adam-Vizi, V. (2000). Exacerbated responses to oxidative stress by an Na⁺ load in isolated nerve terminals: the role of ATP depletion and rise of [Ca²⁺]. *J. Neurosci.* **20**, 2094-2103. doi:10.1523/JNEUROSCI.20-06-02094.2000
- Cole, S. P. C. and Deeley, R. G. (2006). Transport of glutathione and glutathione conjugates by MRP1. *TRENDS in Pharm. Sci.* **27**, 438-446. doi:10.1016/j.tips.2006.06.008
- da Costa, K. M., Valente, R. C., Salustiano, E. J., Gentile, L. B., Freire-de-Lima, L., Mendonça-Previato, L. and Previato, J. O. (2018). Functional characterization of ABCC proteins from *Trypanosoma cruzi* and their involvement with thiol transport. *Front. Microbiol.* **9**, 205. doi:10.3389/fmicb.2018.00205
- Dallas, S., Miller, D. S. and Bendayan, R. (2006). Multidrug resistance-associated proteins: expression and function in the central nervous system. *Pharmacol. Rev.* **58**, 140-161. doi:10.1124/pr.58.2.3
- Dean, M., Rzhetsky, A. and Allikmets, R. (2001). The human ATP-binding cassette (ABC) transporter superfamily. *Genome Res.* **11**, 1156-1166. doi:10.1101/gr.GR-1649R
- DeGorter, M. K., Xia, C. Q., Yang, J. J. and Kim, R. B. (2012). Drug transporters in drug efficacy and toxicity. *Ann. Rev. Pharmacol. Toxicol.* **52**, 249-273. doi:10.1146/annurev-pharmtox-010611-134529
- Della Torre, C., Bocci, E., Focardi, S. E. and Corsi, I. (2014). Differential ABCB and ABCC gene expression and efflux activities in gills and hemocytes of *Mytilus galloprovincialis* and their involvement in cadmium response. *Mar. Environ. Res.* **93**, 56-63. doi:10.1016/j.marenvres.2013.06.005
- Dermauw, W. and Van Leeuwen, T. (2014). The ABC gene family in arthropods: comparative genomics and role in insecticide transport and resistance. *Insect Biochem. Mol. Biol.* **45**, 89-110. doi:10.1016/j.ibmb.2013.11.001
- Elliott, C. J. H. and Kleindienst, H.-U. (1990). Photoinactivation of neurones in the pond snail, *Lymnaea stagnalis*: estimation of a safety factor. *Brain Res.* **524**, 149-152. doi:10.1016/0006-8993(90)90504-5
- Erdő, F. and Krajcsi, P. (2019). Age-Related functional and expression changes in efflux pathways at the blood-brain barrier. *Front. Aging Neurosci.* **11**, 196. doi:10.3389/fnagi.2019.00196
- Erickson, M. A. and Banks, W. A. (2019). Age-associated changes in the immune system and blood-brain barrier functions. *Int. J. Mol. Sci.* **20**, E1632. doi:10.3390/ijms20071632
- Falcão, A. S., Bellarosa, C., Fernandes, A., Brito, M. A., Silva, R. FM., Tiribelli, C. and Brites, D. (2007). Role of multidrug resistance-associated protein 1 expression in the in vitro susceptibility of rat nerve cell to unconjugated bilirubin. *Neurosci.* **144**, 878-888. doi:10.1016/j.neuroscience.2006.10.026
- Fathi-Moghadam, H. and Winlow, W. (2019). Pharmacological dissection of potassium currents in cultured, identified, molluscan neurons. *EC Neuro.* **11.5**, 346-356.
- Featherstone, D. E. (2011). Glial solute carrier transporters in drosophila and mice. *Glia* **59**, 1351-1363. doi:10.1002/glia.21085
- Feng, Z.-P., Zhang, Z., van Kesteren, R. E., Straub, V. A., van Nierop, P., Jin, K., Nejatbakhsh, N., Goldberg, J. I., Spencer, G. E., Yeoman, M. S. et al. (2009). Transcriptome analysis of the central nervous system of the mollusc *Lymnaea stagnalis*. *BMC Genomics.* **10**, 451. doi:10.1186/1471-2164-10-451
- Gekeler, V., Ise, W., Sanders, K. H., Ulrich, W.-R. Beck, J. (1995). The leukotriene LTD4 receptor antagonist MK571 specifically modulates MRP associated multidrug resistance. *Biochem. Biophys. Res. Commun.* **208**, 3453-3452. doi:10.1006/bbrc.1995.1344
- Gott, R. C., Kunkel, G. R., Zobel, E. S., Lovett, B. R. and Hawthorne, D. J. (2017). Implicating ABC transporters in insecticide resistance: research strategies and a decision framework. *J. Econ. Entomol.* **110**, 667-677. doi:10.1093/jee/tox041
- Grube, M., Hagen, P. and Jedlitschky, G. (2018). Neurosteroid transport in the brain: role of ABC and SLC transporters. *Front. Pharmacol.* **9**, 354. doi:10.3389/fphar.2018.00354
- Hagos, F. T., Daood, M. J., Ocque, J. A., Nolin, T. D., Bayir, H., Poloyac, S. M., Kochanek, P. M., Clark, R. S. and Empey, P. E. (2017). Probenecid, an organic anion transporter 1 and 3 inhibitor, increases plasma and brain exposure of N-acetylcysteine. *Xenobiotica* **47**, 346-353. doi:10.1080/00498254.2016.1187777
- Hartz, A. M. and Bauer, B. (2011). ABC transporters in the CNS—an inventory. *Curr. Pharm. Biotechnol.* **12**, 656-673. doi:10.2174/138920111795164020
- Hediger, M. A., Romero, M. F., Peng, J.-B., Rolfs, A., Takanao, H. and Bruford, E. A. (2004). The ABCs of solute carriers: physiological, pathological and therapeutic implications of human membrane transport proteins Introduction. *PLügers Arch.* **447**, 465-468. doi:10.1007/s00424-003-1192-y
- Hermann, P. M. and Bulloch, A. G. M. (1998). Pronase modifies synaptic transmission and activity of identified *Lymnaea* neurons. *Inv. Neurosci.* **3**, 295-304. doi:10.1007/BF02577689
- Hermann, P. M., Lukowiak, K., Wildering, W. C. and Bulloch, A. G. M. (1997). Pronase acutely modifies high voltage-activated calcium currents and cell properties of *Lymnaea* neurons. *Eur. J. Neurosci.* **9**, 2624-2633. doi:10.1111/j.1460-9568.1997.tb01692.x
- Hermann, P. M., Lee, A., Hulliger, S., Minvielle, M., Ma, B. and Wildering, W. C. (2007). Impairment of long-term associative memory in aging snails (*Lymnaea*

- stagnalis*). *Behav. Neurosci.* **121**, 1400-1414. doi:10.1037/0735-7044.121.6.1400
- Hermann, P. M., Watson, S. N. and Wildering, W. C. (2014). Phospholipase A2 – nexus of aging, oxidative stress, neuronal excitability, and functional decline of the aging nervous system? Insights from a snail model system of neuronal aging and age-associated memory impairment. *Front. Genet.* **5**, 419. doi:10.3389/fgene.2014.00419
- Höglund, P. J., Nordström, K. J. V., Schiöth, H. B. and Fredriksson, R. (2011). The solute carrier families have a remarkably long evolutionary history with the majority of the human families present before divergence of Bilaterian species. *Mol. Biol. Evol.* **28**, 1531-1541. doi:10.1093/molbev/msq350
- Janse, C., Slob, W., Popelier, C. M. and Vogelaar, J. W. (1988). Survival characteristics of the mollusc *Lymnaea stagnalis* under constant culture conditions: effects of aging and disease. *Mech. Ageing Dev.* **42**, 263-274. doi:10.1016/0047-6374(88)90052-8
- Jeong, C.-B., Kim, H.-S., Kang, H.-M. and Lee, J.-S. (2017). ATP-binding cassette (ABC) proteins in aquatic invertebrates: Evolutionary significance and application in marine ecotoxicology. *Aquatic Toxicol.* **185**, 29-39. doi:10.1016/j.aquatox.2017.01.013
- Ji, B., Ito, K., Suzuki, H., Sugiyama, Y. and Horie, T. (2002). Multidrug resistance-associated protein2 (MRP2) plays an important role in the biliary excretion of glutathione conjugates of 4-hydroxynonenal. *Free Radic. Biol. Med.* **33**, 370-378. doi:10.1016/S0891-5849(02)00906-1
- Johnston, C. U., Clothier, L. N., Quesnel, D. M., Gieg, L. M., Chua, G., Hermann, P. M. and Wildering, W. C. (2017). Embryonic exposure to model naphthenic acids delays growth and hatching in the pond snail *Lymnaea stagnalis*. *Chemosphere* **168**, 1578-1588. doi:10.1016/j.chemosphere.2016.11.156
- Jungsuwadee, P., Cole, M. P., Sultana, R., Joshi, G., Tangpong, J., Butterfield, D. A., St. Clair, D. K. and Vore, M. (2006). Increase in Mrp1 expression and 4-hydroxy-2-nonenal adduction in heart tissue of Adriamycin-treated C57BL/6mice. *Mol. Cancer Ther.* **5**, 2851-2860. doi:10.1158/1535-7163.MCT-06-0297
- Kuo, M. T. (2009). Redox regulation of multidrug resistance in cancer chemotherapy: molecular mechanisms and therapeutic opportunities. *Antioxid. Redox. Signal.* **11**, 99-133. doi:10.1089/ars.2008.2095
- Lee, J. R. (2019). Mitochondria and fatty acid homeostasis in the aging nervous system. *Ph.D. Thesis*, University of Calgary, Calgary, AB, Canada.
- Lozovaya, N. A., Vulfius, C. A., Ilyin, V. I. and Krasts, I. V. (1993). Intracellular ATP modifies the voltage dependence of the fast transient outward K⁺ current in *Lymnaea stagnalis* neurones. *J. Physiol.* **464**, 441-455. doi:10.1113/jphysiol.1993.sp019644
- Morris, M. E., Rodriguez-Cruz, V. and Felmler, M. A. (2017). SLC and ABC transporters: expression, localization, and species differences at the blood-brain and the blood-cerebrospinal fluid barriers. *AAPS J.* **19**, 1317-1331. doi:10.1208/s12248-017-0110-8
- Nyquist, M. D., Prasad, B. and Mostaghel, E. A. (2017). Harnessing solute carrier transporters for precision oncology. *Molecules* **22**, 539. doi:10.3390/molecules22040539
- Pathak, D., Shields, L. Y., Mendelsohn, B. A., Haddad, D., Lin, W., Gerencser, A. A., Kim, H., Brand, M. D., Edwards, R. H. and Nakamura, K. (2015). The role of mitochondrially derived ATP in synaptic vesicle recycling. *J. Biol. Chem.* **290**, 22325-22336. doi:10.1074/jbc.M115.656405
- Rangaraju, V., Calloway, N. and Ryan, T. A. (2014). Activity-driven local ATP synthesis is required for synaptic function. *Cell* **156**, 825-835. doi:10.1016/j.cell.2013.12.042
- Renes, J., de Vries, E. G., Nienhuis, E. F., Jansen, P. L. M. and Müller, M. (1999). ATP- and glutathione-dependent transport of chemotherapeutic drugs by the multidrug resistance protein MRP1. *Br. J. Pharmacol.* **126**, 681-688. doi:10.1038/sj.bjp.0702360
- Renes, J., de Vries, E. E., Hooiveld, G. J., Krikken, I., Jansen, P. L. and Müller, M. (2000). Multidrug resistance protein MRP1 protects against the toxicity of the major lipid peroxidation product 4-hydroxynonenal. *Biochem. J.* **350**, 555-561. doi:10.1042/bj3500555
- Rosenecker, D., Wright, C. and Lukowiak, K. (2010). A quantitative proteomic analysis of long-term memory. *Mol. Brain* **3**, 9. doi:10.1186/1756-6606-3-9
- Salerno, M. and Garnier-Suillerot, A. (2001). Kinetics of glutathione and daunorubicin efflux from multidrug resistance protein overexpressing small-cell lung cancer cells. *Eur. J. Pharmacol.* **421**, 1-9. doi:10.1016/S0014-2999(01)00992-X
- Slob, W. and Janse, C. (1988). A quantitative method to evaluate the quality of interrupted animal cultures in aging studies. *Mech. Ageing Dev.* **42**, 275-290. doi:10.1016/0047-6374(88)90053-X
- Song, L., Hennink, E. J., Young, T. and Tanke, H. J. (1995). Photobleaching kinetics of fluorescein in quantitative fluorescence microscopy. *Biophys. J.* **68**, 2588-2600. doi:10.1016/S0006-3495(95)80442-X
- Sultana, R. and Butterfield, D. A. (2004). Oxidatively modified GST and MRP1 in Alzheimer's disease brain: implications for accumulation of reactive lipid peroxidation products. *Neurochem. Res.* **29**, 2215-2220. doi:10.1007/s11064-004-7028-0
- Valdez, B. C., Hassan, M. and Andersson, B. S. (2017). Development of an assay for cellular efflux of pharmaceutically active agents and its relevance to understanding drug interactions. *Exp. Hematol.* **52**, 65-71. doi:10.1016/j.exphem.2017.04.011
- Van der Kolk, D. M., de Vries, E. G., Koning, J. A., van den Berg, E., Muller, M. and Vellenga, E. (1998). Activity and expression of the multidrug resistance proteins MRP1 and MRP2 in acute myeloid leukemia cells, tumor cell lines, and normal hematopoietic CD34⁺ peripheral blood cells. *Clin. Cancer Res.* **4**, 1727-1736. doi:10.1038/sj.leu.2402236
- Watson, S. N., Nelson, M. A. and Wildering, W. C. (2012a). Redox agents modulate neuronal activity and reproduce physiological aspects of neuronal aging. *Neurobiol. Aging* **33**, 149-161. doi:10.1016/j.neurobiolaging.2010.01.017
- Watson, S. N., Risling, T. E., Hermann, P. M. and Wildering, W. C. (2012b). Failure of delayed nonsynaptic neuronal plasticity underlies age-associated long-term associative memory impairment. *BMC Neurosci.* **13**, 103. doi:10.1186/1471-2202-13-103
- Watson, S. N., Wright, N., Hermann, P. M. and Wildering, W. C. (2013). Phospholipase A2: the key to reversing long-term memory impairment in a gastropod model of aging. *Neurobiol. Aging* **34**, 610-620. doi:10.1016/j.neurobiolaging.2012.02.028
- Watson, S. N., Lee, J. R., Risling, T. E., Hermann, P. M. and Wildering, W. C. (2014). Diminishing glutathione availability and age-associated decline in neuronal excitability. *Neurobiol. Aging* **35**, 1074-1085. doi:10.1016/j.neurobiolaging.2013.11.007
- Willers, C., Svitina, H., Rossouw, M. J., Swanepoel, R. A., Hamman, J. H. and Gouws, C. (2019). Models used to screen for the treatment of multidrug resistant cancer facilitated by transporter-based efflux. *J. Cancer Res. Clin. Oncol.* **145**, 1949-1976. doi:10.1007/s00432-019-02973-5
- Yamazaki, M., Li, B., Louie, S. W., Pudvah, N. T., Stocco, R., Wong, W., Abramovitz, M., Demartis, A., Laufer, R., Hochman, J. H. et al. (2005). Effects of fibrates on human organic anion-transporting polypeptide 1B1-, multidrug resistance protein 2- and P-glycoprotein-mediated transport. *Xenobiotica* **35**, 737-753. doi:10.1080/00498250500136676
- Zhang, H. and Forman, H. J. (2017). 4-hydroxynonenal-mediated signaling and aging. *Free Radic. Biol. Med.* **111**, 219-225. doi:10.1016/j.freeradbiomed.2016.11.032